Modelling near-surface soil temperature and moisture for germination response predictions of post-wildfire seedbeds

G.N. Flerchinger*, S.P. Hardegree

USDA Agricultural Research Service, Northwest Watershed Research Center, 800 Park Blvd., Plaza IV, Suite 105, Boise, ID 83712, USA

Abstract

A major contributor to degradation on rangelands in the western United States is the expansion of undesirable annual weeds following wildfire or other disturbance. The Simultaneous Heat and Water (SHAW) model was applied to three soil types (loamy sand, sandy loam, and silt loam) to simulate near-surface soil temperature and water for predicting potential seed germination in post-wildfire revegetation. Three parameterization methods including initial parameter estimates, calibrated parameters, and measured moisture-release curve parameters were compared to assess the effect of parameter uncertainty on germination prediction. Initial parameters for the sandy loam soil resulted in an underprediction of germination times by 4.7 days for cheatgrass to 12.8 days for bluebunch wheatgrass compared to germination estimated from measured soil temperature and water conditions. Initial parameters resulted in predicted germination within 2 days of estimates for the other two soils. Model calibration to optimize the surface 20-cm water-content did not necessarily improve predicted germination. Model simulations using measured moisture-release curves resulted in germination prediction within a few days relative to estimates for all sites. Results suggest that the model can be used for long-term simulations of seedbed microclimate necessary to evaluate potential germination response of revegetation species and their weedy competitors.
Published by Elsevier Ltd.

Keywords: Rangeland restoration; Soil water potential; Soil water-content; SHAW model; Model calibration; Invasive species

*Corresponding author. Tel.: +1-208-422-0716; fax: +1-208-334-1502.
E-mail address: gflerchi@nwrc.ars.usda.gov (G.N. Flerchinger).

1. Introduction

Rangelands comprise about 55% of the total land area of the United States and about 80% of the 17 western states. Resource values are impaired or threatened on millions of acres of these rangelands because of the expansion of undesirable non-native annual weeds following wildfire or other disturbance (Young and Longland, 1996). Opportunistic weedy species are especially well suited to take advantage of ecosystem disturbance and changes in climate. New methodologies must be developed to determine the sequence of management actions that will result in the reestablishment of viable, persistent and appropriately diverse plant communities on the western rangelands.

Critical factors determining the success of seeding efforts are the spatial and temporal distribution of soil temperature and moisture relative to the growth response of both desirable plant species and weedy competitors (Roundy and Call, 1988). Microclimatic requirements for seedling establishment are much more restrictive than the conditions necessary for persistence of mature perennial vegetation as reflected in current seeding guides. Seedbed microclimate is determined by soils, vegetation and atmospheric interaction that exhibit high spatial and temporal variability (Call and Roundy, 1991; Pierson and Wight, 1991). We cannot predict the system requirements for plant community establishment until we are able to characterize the spatial and temporal variability in microclimatic conditions in the field for both vegetated and bare-soil conditions. Current technology permits continuous monitoring of the temperature and water regime of the seedbed, but due to the intensive effort required to continuously monitor soil variables, such data are extremely limited.

Computer simulation is a potentially valuable tool for arid land revegetation (McDonald, 2002) and characterization of historical and potential future patterns of seedbed microclimate (Hardegree et al., 2003). Seedbed microclimatic conditions are difficult to accurately simulate due to uncertainty in soil parameters and rapid changes in near-surface conditions in response to atmospheric conditions. The majority of soil water and temperature models primarily address agricultural lands and have not been validated for simulating wildland seedbed conditions. Objectives of this paper were to: determine the impact of uncertainty in input soil parameters on the predicted germination time of rangeland grasses, and determine the feasibility of driving a germination response model with a soil-microclimate model for the purpose of generating long-term historical simulations of seedbed temperature and moisture. Near-surface soil temperature and water were simulated on three soil types using three parameterization schemes. Soil model output was evaluated by assessing the potential impact on seed germination response of three rangeland grasses relative to that estimated from measured soil parameters.

2. SHAW model description

The Simultaneous Heat and Water (SHAW) Model is a one-dimensional model originally developed to simulate soil freezing and thawing (Flerchinger and Saxton,

1989). The ability of the model to simulate heat and water movement through plant cover, snow, residue and soil has been demonstrated for predicting climate and management effects on soil freezing (Flerchinger and Saxton, 1988; Flerchinger and Hanson, 1989; Xu et al., 1991; Hayhoe, 1994; Flerchinger and Seyfried, 1997; Kennedy and Sharratt, 1998), snowmelt (Flerchinger et al., 1994, 1996a), soil temperature, soil water (Flerchinger and Pierson, 1991; Hymer et al., 2000; McDonald, 2002), evapo-transpiration and water balance (Flerchinger et al., 1996b, 1998; Parkin et al., 1999).

The SHAW model simulates a one-dimensional vertical profile extending from the top of a plant canopy or the snow, residue or soil surface to a specified depth within the soil. Weather conditions above the upper boundary and soil conditions at the lower boundary define heat and water fluxes into the system. Water and heat flux at the surface boundary include absorbed solar radiation, long-wave radiation exchange, and turbulent transfer of heat and vapor. Absorbed solar radiation, corrected for local slope, is based on measured incoming short-wave radiation and includes reflection and back-scattering within the canopy and residue layers. Long-wave radiation emitted by the atmosphere is estimated from the Stefan–Boltzmann law and adjusted for cloud cover (estimated from measured solar radiation). Surface sensible and latent heat transfer is estimated using a bulk aerodynamic approach with stability corrections.

Soil water flux in the model is computed using an implicit solution of the Richards equation. The relation assumed for the soil water characteristic equation is (Campbell, 1974)

$$\psi = \psi_e \left(\frac{\theta}{\theta_s}\right)^{-b},\qquad(1)$$

where ψ_e is air entry potential (bars), b is a pore size distribution parameter, θ is liquid water-content ($m^3 m^{-3}$), and θ_s is saturated water-content ($m^3 m^{-3}$). Unsaturated hydraulic conductivity in the SHAW model is computed from (Campbell, 1974)

$$K = K_s \left(\frac{\theta}{\theta_s}\right)^{(2b+3)},\qquad(2)$$

where K_s is saturated hydraulic conductivity ($m s^{-1}$).

3. Field description

The SHAW model was tested using data collected at the Orchard Field Test Site located in south-western Idaho ($43°19'N$, $115°59'W$). The site is relatively flat and receives approximately 293 mm of precipitation annually. Vegetation at the site is dominated by cheatgrass (*Bromus tectorum* L.) which has invaded the native sagebrush rangeland. Soils are quite variable; three microclimatic monitoring sites were established within 400 m of each other, one in each of three soil types: loamy sand, sandy loam, and silt loam. Each monitoring site consists of six plots, three

maintained for bare soil and three maintained for annual cheatgrass cover. This study focuses on the bare soil plots, which are maintained to approximate post-burn conditions.

Soil temperature and water sensors were installed at each of the plots by excavating a pit, installing sensors horizontally from the face of the pit and replacing the soil by horizons. Thermocouples recorded hourly soil temperature at depths of 1, 2, 5, 10, 20, 30, 50 and 100 cm in each plot. Soil water was recorded at these same depths, except for the 1 cm depth, using 3-prong 20-cm time domain reflectometry (TDR) probes read every two hours by a Trase waveguide analyzer (Soil Moisture Inc., Santa Barbara, CA). Meteorologic stations at each of the three sites collected air temperature, precipitation, wind speed, humidity, and solar radiation.

Soil properties are summarized for the bare plots at each site in Table 1. Soil textural analysis was conducted by hydrometer method on three samples from each of the six pits at 10-cm intervals to a depth of 100 cm in addition to a 5-cm sample. Soil density was measured from gravimetric core samples taken at these same depths. Sites A and B are classified within the Tindahay series (sandy, mixed, mesic Xeric Torriorthents); site A is a Tindahay loamy sand and Site B is a Tindahay sandy loam. Texture of site A is quite uniform for the entire 100-cm profile sampled, with sand content near 90%. Site B is relatively uniform to a depth of approximately 75 cm, below which soil texture is similar to site A. Site C is classified as a Lankbush silt loam (fine-loamy, mixed, superactive, mesic Xeric Haplargids) and is the most heterogenous of the three sites.

Pressure plate analyses were conducted on disturbed soil surface (<20 cm) samples collected from each of the three sites to determine moisture-release curves. Soil samples were sieved and compacted into 65-mm diameter by 50-mm rings for pressure plate analysis. Water-content measurements were taken at 11 water potential settings ranging from 0.1 to 15 bar.

Table 1
Measured soil textures and densities

	Depth (cm)	Sand (%)	Silt (%)	Clay (%)	Density (kg m^{-3})
Site A	0–5	90	8	2	1624
	5–20	86	10	4	1656
	20+	92	4	4	1723
Site B	0–5	75	20	5	1435
	5–20	71	21	8	1616
	20–75	78	16	6	1568
	75+	89	7	4	1536
Site C	0–5	36	51	13	1180
	5–25	36	51	13	1322
	25–50	23	62	15	1368
	50–65	41	49	10	1510
	65+	61	33	6	1544

4. Model application

When used as a tool for historical or potential future seedbed conditions, the model will likely be initialized in the fall following the fire season when water-content is typically near the minimum residual water-content under regional climatic conditions (Hardegree et al., 2003). Thus, simulation of spring germination conditions after accounting for overwinter processes is critical. Soil temperature and water were therefore simulated from early October (day 279) of 1994 through the spring germination period ending in late May (day 150). Simulation results were compared with measured soil temperature and water-content for the seedling germination period from March through May (day 60–150) of 1995 using model efficiency (ME), root mean square difference (RMSD) and mean bias error (MBE). Definitions for each are given in Table 2 (Nash and Sutcliffe, 1970; Green and Stephenson, 1986).

Bare soil conditions were assumed for each of the three sites. Simulations were conducted to a depth of 4 m, where moisture content and temperature were assumed constant. The model was initialized with measured soil temperature and water-content to a depth of 1 m and extrapolated conditions to a depth of 4 m.

Because measured soil hydraulic parameters are seldom available in a revegetation scenario, moisture-release curve parameters and saturated hydraulic conductivity were estimated based on soil texture and bulk density using the SHAW model user interface. The user interface uses relations described by Campbell (1985) to estimate moisture-release curve parameters and by Saxton et al. (1986) for saturated conductivity. Soil hydraulic parameters were subsequently calibrated to measure soil water-contents for the germination period. Simulations were also conducted using input parameters derived from pressure plate measurements. Initial estimated parameters, calibrated parameters, and parameters obtained from the pressure plate measurements are given in Table 3. Parameters in Table 3 were considered applicable as deep as the surface soil texture could be considered relatively homogeneous, i.e. 100 cm for site A, 75 cm for site B and 25 cm for site C (Table 1). Parameters for deeper depths were estimated using the SHAW model user interface.

Table 2
Description and definition of model performance measures

Measure	Description	Mathematical definition[a]
ME	Model efficiency, i.e. variation in measured values accounted for by the model.	$1 - \dfrac{\sum_{i=1}^{N}(Y_i - \hat{Y}_i)^2}{\sum_{i=1}^{N}(Y_i - \bar{Y})^2}$
RMSD	Root mean square difference between simulated and observed values.	$\left[\dfrac{1}{N}\sum_{i=1}^{N}(\hat{Y}_i - Y_i)^2\right]^{1/2}$
MBE	Mean bias error of model predictions compared to observed values.	$\dfrac{1}{N}\sum_{i=1}^{N}(\hat{Y}_i - Y_i)$

[a] $\hat{Y}_i$ = simulated values; Y_i = observed values; $\bar{Y}$ = mean of observed values; N = number of observations.

Table 3
Initial estimates, calibrated values and pressure plate measurements of the surface soil hydraulic parameters[*] for each site

		θ_s (m^3 m^{-3})	b	ψ_e (bar)	K_s (cm h^{-1})
Site A	Initial estimates	0.39	3.82	−0.007	12.24
	Calibrated parameters	0.32	3.82	−0.009	12.24
	Pressure plate parameters	0.39	3.16	−0.013	n/a[a]
Site B	Initial estimates	0.46	4.16	−0.011	6.10
	Calibrated parameters	0.46	4.16	−0.033	6.10
	Pressure plate parameters	0.46	3.24	−0.044	n/a[a]
Site C	Initial estimates	0.55	4.09	−0.034	1.98
	Calibrated parameters	0.55	4.09	−0.034	0.99
	Pressure plate parameters	0.55	3.51	−0.061	n/a[a]

[*] $\psi = \psi_e \left(\dfrac{\theta}{\theta_s} \right)^{-b}$.

[a] K_s from calibrated runs was used for simulations using pressure plate parameters.

4.1. Initial parameters

Simulated and measured daily soil temperature during the germination period (day 60–150) for the 2- and 50-cm depths at site C are plotted in Fig. 1. ME for the 2-cm depth was 0.90, 0.89, and 0.96 for sites A, B, and C, respectively. RMSD for the three sites was 1.54°C, 1.06°C, and 0.92°C, respectively. In general, ME and RMSD for simulated temperatures improved with depth, but MBE increased with depth. RMSD at the 100-cm depth ranged from 0.26°C to 0.48°C, and ME approached 0.99. Soil temperatures were slightly underpredicted for site A, with the MBE ranging from −0.08°C to −1.14°C. At site B, MBE ranged from +0.05°C for the 1-cm depth to +0.42°C for the 50-cm depth. MBE for site C ranged from +0.01 for the 1-cm depth to −0.61 at 100-cm.

The RMSD for simulated hourly soil temperature at site A was highest for the 1-cm depth, with a value of 3.35°C and decreased with depth to a low of 0.28°C at the 100-cm depth. ME was 0.72 for the 1-cm depth and 0.99 for the 100-cm depth. Values RMSD for the soil profile at sites B and C were similar to that for site A, but near-surface ME was slightly lower with values of 0.67 and 0.62 for sites B and C.

Temporal changes in near-surface soil moisture in response to the timing of precipitation is critical for seed germination. Measured and simulated daily average 2-cm soil water-content (2) for the three sites is plotted along with precipitation in Fig. 2. Soils were relatively moist on day 65, but dried continually until approximately day 120, interrupted only by a few small precipitation events. Several large precipitation events wet the soil substantially following day 120, returning soil water conditions more favorable for germination. The temporal changes in water-content were simulated relatively well for sites A and C, but site B dried sooner than
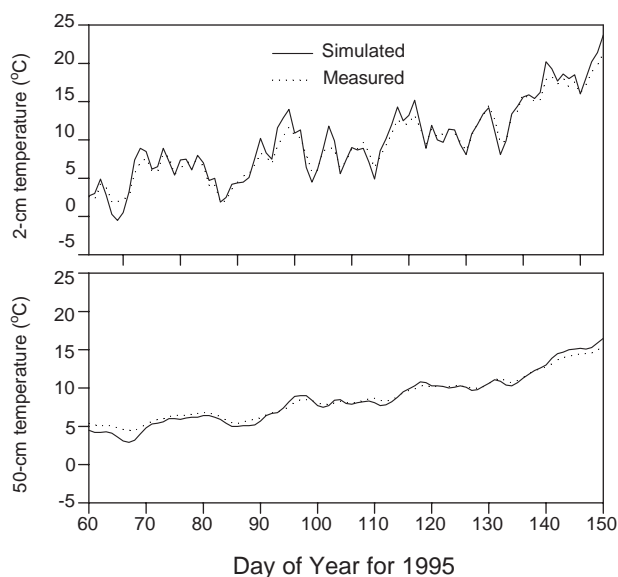
Fig. 1. Simulated and measured daily soil temperature during the germination period for the 2- and 50-cm depths at site C for the simulation using initial parameter estimates.

simulated. RMSD for the hourly 2-cm simulated soil water-content compared to the TDR measurements during the germination period was 0.032, 0.046, and $0.022 \, m^3 \, m^{-3}$ for sites A, B and C, respectively, as shown in Table 4. The average RMSD for the surface 20-cm was $0.022 \, m^3 \, m^{-3}$ for site A, $0.045 \, m^3 \, m^{-3}$ for site B and $0.024 \, m^3 \, m^{-3}$ for site C. In general, water-content for sites A and B was slightly overpredicted near the surface and underpredicted at deeper depths. Water-content tended to be underpredicted for the entire profile at site C.

4.2. Sensitivity analysis

No calibrations or sensitivity analyses were performed for soil temperature, since these were simulated reasonably well. Sensitivity of simulations to perturbations in soil hydraulic parameters were evaluated as a first step in calibration. Soil hydraulic parameters were calibrated to optimize simulated water-content within the top 20 cm, i.e. the area most critical for seedling germination and plant establishment. The hydraulic parameters were calibrated in an iterative fashion. Initially, each soil hydraulic parameter was varied independently to determine which parameter could minimize the average RMSD for the soil water-content within the top 20 cm. For each subsequent iteration, all remaining parameters were varied while holding constant the parameter which minimized the average RMSD in the previous iteration. In most cases, no further reduction in RMSD was obtained after the first iteration.
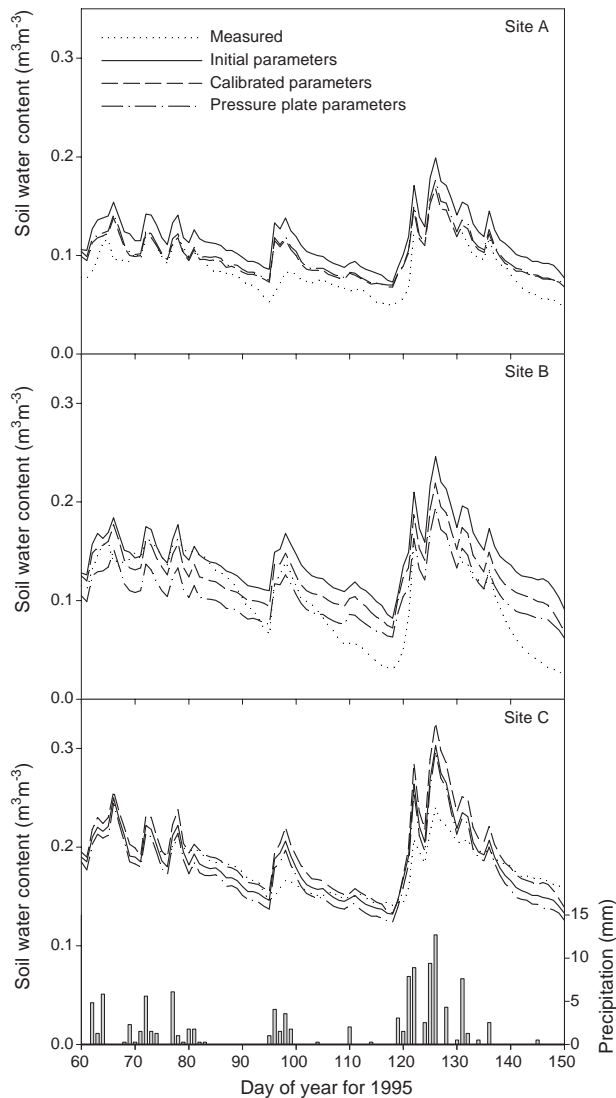
Fig. 2. Precipitation, measured 2-cm soil water-content and simulation results using the initial parameter estimates, calibrated parameters, and parameters obtained from pressure plate measurements for: the loamy sand site A; the sandy loam site B; and the silt loam site C.

Results from the initial calibration step are presented in Fig. 3 for the three sites. Simulation results are most sensitive to saturated water-content (θ_s) and pore-size distribution index (b) for all three sites. The curves for site C suggest that these two parameters are very near their optimum values, as both curves reach a minimum near the initial values. The slope for all parameters at the initial values is opposite for

Table 4
Model performance measures for soil water content simulations using initial estimates of hydraulic parameters, calibrated parameters, and parameters obtained from pressure plate measurements

		Average RMSD for surface 20 cm ($m^3\,m^{-3}$)	2-cm RMSD ($m^3\,m^{-3}$)	2-cm ME
Site A	Initial estimates	0.022	0.032	−1.22
	Calibrated parameters	0.014	0.018	0.26
	Pressure plate parameters	0.014	0.020	0.09
Site B	Initial estimates	0.045	0.046	−0.11
	Calibrated parameters	0.034	0.033	0.43
	Pressure plate parameters	0.033	0.028	0.57
Site C	Initial estimates	0.024	0.022	0.17
	Calibrated parameters	0.020	0.028	−0.34
	Pressure plate parameters	0.029	0.023	0.12

site C compared to the other two sites. This is likely due to the fact that near-surface water-content was overpredicted for sites A and B and underpredicted for site C. Thus, any change that would promote downward water flux would decrease the average RMSD for sites A and B and increase RMSD for site C. Based on Eq. (2) for a given water-content, unsaturated conductivity, K, will strongly decrease with an increase in either b or θ_s, while K_s produces only a linear change. Interestingly, equal changes in K_s and ψ_e produced nearly identical changes in soil water-content. However, this was not the case for simulated soil water potential. Changes in ψ_e resulted in much larger changes in simulated water potential than in K_s (not shown).

4.3. Calibrated parameters

Parameter calibration reduced the average RMSD of the surface 20-cm water-content for the three sites from 0.022, 0.045 and 0.024 $m^3\,m^{-3}$ to 0.014, 0.034, and 0.020 $m^3\,m^{-3}$, respectively (Table 4). This change had mixed results on the hourly 2-cm soil water-content; RMSD for sites A and B decreased by 0.014 and 0.013 $m^3\,m^{-3}$, but site C increased by 0.006 $m^3\,m^{-3}$.

Changes in simulated temperature resulting from the moisture calibration were minor. RMSD for the calibrated simulation changed less than $0.03\,°C$ compared to the initial simulation for all three sites. MBE for the 2-cm depth changed by $-0.12\,°C$, $-0.18\,°C$ and $+0.14\,°C$.

4.4. Pressure plate parameters

Values of K_s from the calibrated simulations were used in the simulations using moisture-release curve parameters based on pressure plate measurements. Soil
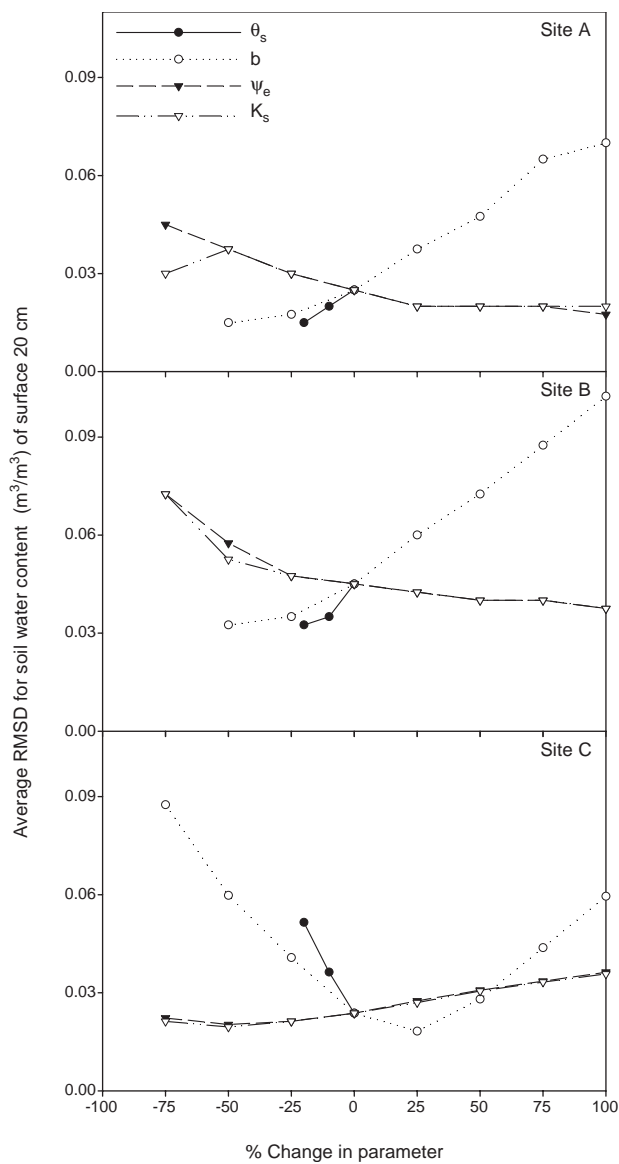
Fig. 3. Sensitivity of simulated water-content to changes in the absolute value of the initial soil hydraulic parameters; θ_s is saturated water-content, b is pore-size distribution index, ψ_e is air entry potential, and K_s is saturated hydraulic conductivity. Sensitivity is based on the average root-mean-square deviation (RMSD) between simulated and measured soil water-content for the 2, 5, 10 and 20 cm soil depths.

water-content from these simulations resulted in the surface 20-cm RMSD, for sites A and B, being very near to that for the calibrated runs (Table 4). Values for the three sites were 0.014, 0.033, and 0.029 $m^3\,m^{-3}$, respectively. Although the average

20-cm RMSD for site C was somewhat higher compared to the calibrated run, both RMSD and ME for the 2-cm depth improved.

5. Impact of modelling uncertainty on germination

It was shown that simulated soil water-content can vary moderately depending on the method of parameter estimation, resulting in uncertainty in simulation results. Thus, it is imperative to discern the impact of this uncertainty on predicted germination. Hardegree et al. (2003) developed response curves for selected rangeland grass species as a function of temperature and water potential. An example of a germination response curve is plotted in Fig. 4.

Soil water potential (P), which is more directly related to germination than soil water-content, is plotted for each of the simulations in Fig. 5. Also plotted is an estimated soil water potential based on Eq. (1) using measured soil water-content and the measured moisture-release parameters. Small differences in soil water-content plotted in Fig. 2 can result in substantial differences in simulated soil water potential due to differences in the moisture-release parameters used in the simulations. Variations between simulated water potential for site B are quite large, with the simulation from the initial parameters having a considerably higher potential (less negative) than the other simulations. Simulations for site A are quite similar, but the overprediction in soil water-content (Fig. 2a) compared to measurements is quite evident in the simulated soil water potential (Fig. 5a).
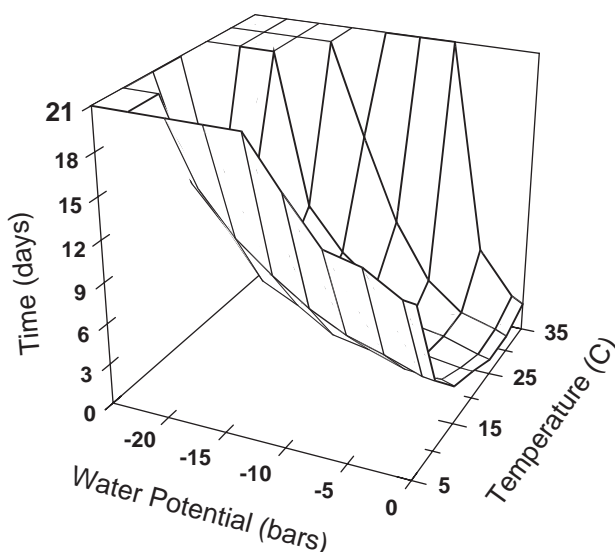

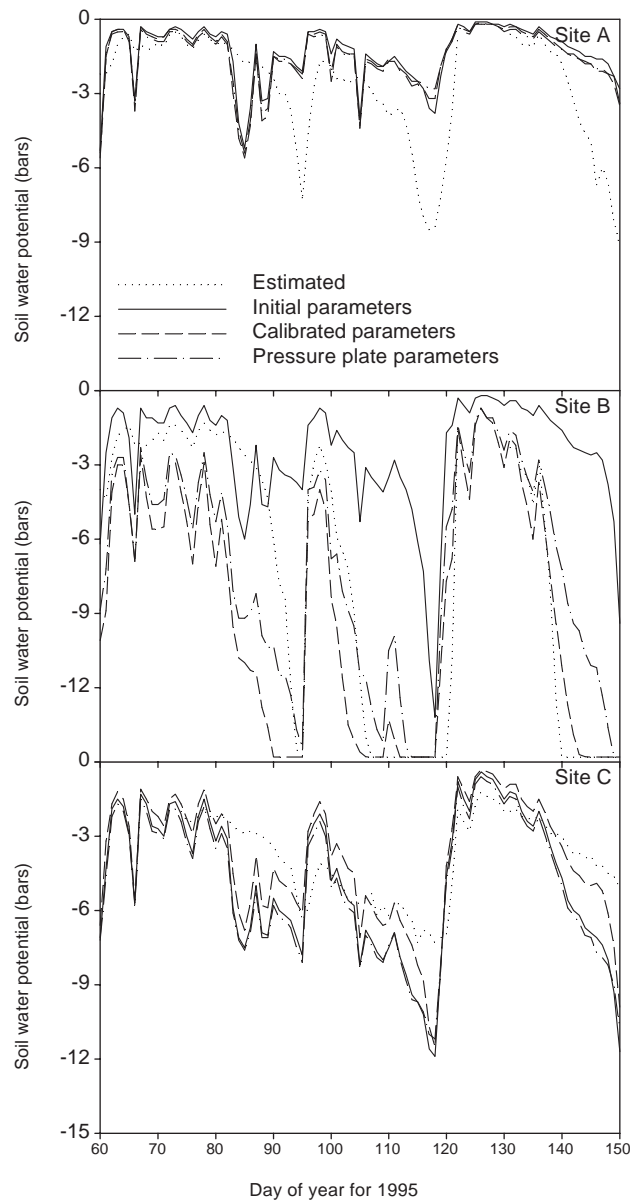Fig. 4. Germination response time for bluebunch wheatgrass.

Fig. 5. Estimated soil water potential at the 2-cm depth and simulation results using the initial parameter estimates, calibrated parameters, and parameters obtained from pressure plate measurements for: the loamy sand site A; the sandy loam site B; and the silt loam site C. (Estimated water potential was calculated from measured water-content using moisture-release curves from disturbed samples.)

Using response curves developed by Hardegree et al. (2003) similar to that plotted in Fig. 4, time required for germination for each day during the germination period was estimated from measured and simulated 2-cm soil temperature and water potential for three grass species cheatgrass (*Bromus tectorum* L.), big squirreltail [*Elymus multisetus* (J.G. Smith) M.E. Jones] and bluebunch wheatgrass [*Pseudoroegneria spicata* (Pursh) Löve]. Cheatgrass germinates relatively quickly and is less susceptible to dry and cold conditions than the other two species. Instantaneous germination rates were estimated for each hour using a 50% germination response model. When the summation of the instantaneous germination rates reached 1.0, 50% of the seedlot was assumed to have germinated. Summations were initiated on each day between day 60 and 150 to determine the time required for germination for each possible planting date during the germination period.

Soil temperature was simulated reasonably well for all three sites. Thus, the limitation to accurate germination prediction was the accuracy of the soil moisture simulation. Predicted time required for germination based on the initial simulations is plotted against estimated germination time in Fig. 6. Germination predictions for site A, the loamy sand, were very similar for all three simulations (Table 5), as there was very little difference in the simulated water potential (Fig. 5). Overprediction of soil water potential did not adversely impact germination prediction because the estimated water potential did not become dry enough to significantly deter germination. The initial simulation for site B, the sandy loam site, was too wet, resulting in germination being underpredicted by an average of 4.7 days for cheatgrass and up to 12.8 days for bluebunch wheatgrass. Germination prediction improved considerably for this site when using the calibrated or the pressure plate parameters, as shown in Table 4; MBE went from −4.7 days for cheatgrass to −1.1 days, and ME went from negative values to as high as 0.91. Germination predictions for the initial simulation of site C compared better with estimated germination than the calibrated simulation because the simulation for the 2-cm depth did not improve with calibration to the surface 20 cm. Germination predictions using pressure plate parameters for site C were similar to the initial simulation.

6. Summary and conclusions

Germination time for three common grass species (cheatgrass, big squirreltail, and bluebunch wheatgrass) on three soil types was predicted from a germination response model using temperature and water conditions simulated by the SHAW model. Model comparisons were conducted for simulations based on initial estimates of soil hydraulic parameters, calibrated parameters from a sensitivity analysis, and moisture-release curve parameters obtained from pressure plate measurements on disturbed soil samples. Simulated soil temperature and water-content were compared with measured soil temperature and water-content. Soil temperature was simulated relatively accurately for all sites. Thus, the limitation in the prediction of germination time was accurate simulation of soil water conditions.
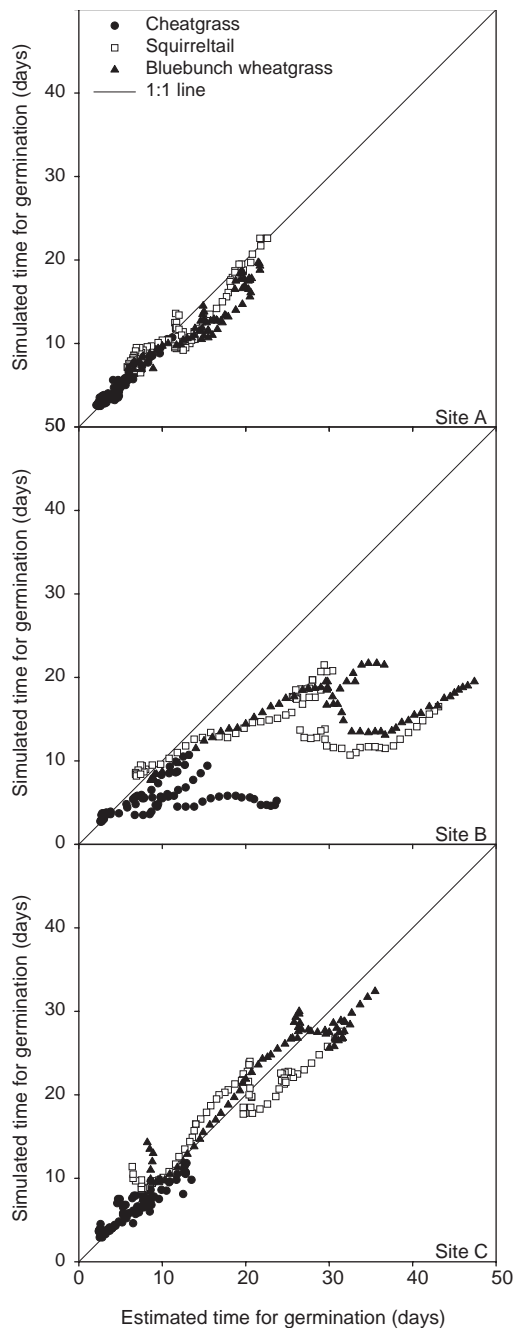
Fig. 6. Predicted germination time based on simulations from the initial parameter estimates versus estimated germination time for: the loamy sand site A; the sandy loam site B; and the silt loam site C.

Table 5

Average estimated germination time and mean bias error (days) between simulated and estimated germination for three grass species[a] using initial estimates of hydraulic parameters, calibrated parameters, and parameters obtained from pressure plate measurements (Numbers in parentheses are model efficiencies)

	Site A			Site B			Site C		
	Brte	Elmu	Pssp	Brte	Elmu	Pssp	Brte	Elmu	Pssp
Average germination	4.9	12.8	14.3	10.1	24.4	28.1	6.7	17.0	21.0
Initial estimates	0.0	−0.4	−2.0	−4.7	−10.6	−12.8	−0.3	−0.1	−0.2
	(0.95)	(0.87)	(0.71)	(−0.51)	(−0.83)	(−0.87)	(0.82)	(0.86)	(0.91)
Calibrated parameters	+0.1	−0.1	−1.2	+1.3	+5.2	+6.7	−0.9	−1.8	−3.0
	(0.94)	(0.87)	(0.79)	(0.77)	(0.28)	(−0.06)	(0.73)	(0.74)	(0.71)
Pressure plate	+0.2	−0.1	−1.2	−1.1	+1.3	+2.1	−0.1	+0.6	+1.0
	(0.93)	(0.87)	(0.78)	(0.66)	(0.91)	(0.82)	(0.86)	(0.87)	(0.91)

[a] Brte is cheatgrass, Elmu is big squirreltail, and Pssp is bluebunch wheatgrass.

Simulated soil water-content and soil water potential for the three simulations on site A were very similar (Figs. 3a and 5a). Due to the sandy nature and homogeneity of this site, soil input parameters could be estimated more accurately than the other sites, resulting in relatively accurate and consistent results between the three simulations. Measured moisture-release curves from disturbed samples likely represent field conditions better for this site due to the lack of any significant soil structure in this sandy soil.

Although the model was able to track temporal changes in measured soil water-content for sites A and C, near-surface soil at site B dried somewhat quicker than any of the simulations for site B. This resulted in the near-surface soil water potential being overpredicted (less negative) for site B using the initial parameter estimates. However, soil water potential using the calibrated and measured parameters tracked estimated soil water potential relatively well.

Results for simulated soil water-content at site C were mixed. Calibration to optimize the upper 20-cm soil water-content resulted in poorer estimates for the 2-cm soil water. Perhaps this is due to the increased heterogeneity of this site. The simulation using the initial estimated parameters produced simulated 2-cm soil water-contents which agreed most favorably with measured values, but only slightly better than the simulation using pressure plate parameters.

With the exception of the initial simulation for site B, predicted germination times were simulated with a ME better than 0.70 in most instances and RMSD less than 5 days. In most cases, germination was predicted best for cheatgrass, which germinates relatively quickly and is less affected by cold and dry soil conditions. In almost all cases, the MBE for predicted germination was lowest for cheatgrass. However, because germination time varies more for squirreltail and bluebunch wheatgrass, ME, which is a measure of the variability explained by the model, was sometimes better for these grasses.

Based on simulation results, the SHAW model can be used in conjunction with a seedling germination model to give reliable predictions of germination times for most instances. Obviously the reliability depends on the accuracy of input parameters. The difference in average germination time between the initial simulation and that using measured moisture-release curve parameters for the three grass species was less than 0.8 days for site A and 1.2 for site C. However, the difference for site B ranged from 3.6 days for cheatgrass to 14.9 days for bluebunch wheatgrass. A difference for 1–5 days in predicted germination time will likely not effect any management decision with respect to a revegetation scenario. However, a difference of 15 days may alter a decision as to whether the bluebunch wheatgrass should be planted. Thus, careful selection of input parameters is essential. Based on these results, model simulations can be used to assess year-to-year variability in germination response for these rangeland grasses using long-term weather conditions, as conducted by Hardegree et al. (2003).

References

Call, C.A., Roundy, B.A., 1991. Perspectives and processes in revegetation of arid and semiarid rangelands. Journal of Range Management 44, 543–549.

Campbell, G.S., 1974. A simple method for determining unsaturated conductivity from moisture retention data. Soil Science 117 (6), 311–314.

Campbell, G.S., 1985. Soil Physics with BACIC: Transport Models for Soil–Plant Systems. Elsevier Science Publishers, Amsterdam, 150pp.

Flerchinger, G.N., Hanson, C.L., 1989. Modeling soil freezing and thawing on a rangeland watershed. Transactions of ASAE 32 (5), 1551–1554.

Flerchinger, G.N., Pierson, F.B., 1991. Modeling plant canopy effects on variability of soil temperature and water. Agricultural and Forest Meteorology 56, 227–246.

Flerchinger, G.N., Saxton, K.E., 1988. Modeling tillage and residue effects on the hydrology of agricultural croplands. In: Modeling Agricultural, Forest, and Rangeland Hydrology. Proceeding of the International Symposium, ASAE Publication 07-88. American Society of Agricultural Engineers, St. Joseph, MI, pp. 176–185.

Flerchinger, G.N., Saxton, K.E., 1989. Simultaneous heat and water model of a freezing snow–residue–soil system I. Theory and development. Transactions of ASAE 32 (2), 565–571.

Flerchinger, G.N., Seyfried, M.S., 1997. Modeling Soil Freezing and Thawing and Frozen Soil Runoff with the SHAW Model. In: Iskandar, I.K., Wright, E.A., Radke J.K., Sharratt, B.S., Groenevelt, P.H., Hinzman, L.D. (Eds.), Proceedings of the International Symposium on Physics, Chemistry, and Ecology of Seasonally Frozen Soils, Fairbanks, AK, June 10–12, 1997, CRREL Special Report 97-10. US Army Cold Regions Research and Engineering Laboratory, Hanover, NH, pp. 537–543.

Flerchinger, G.N., Cooley, K.R., Deng, Y., 1994. Impacts of spatially and temporally varying snowmelt on subsurface flow in a mountainous watershed: 1. Snowmelt simulation. Hydrological Science Journal 39 (5), 507–520.

Flerchinger, G.N., Baker, J.M., Spaans, E.J.A., 1996a. A test of the radiative energy balance of the SHAW model for snowcover. Hydrological Processes 10 (10), 1359–1367.

Flerchinger, G.N., Hanson, C.L., Wight, J.R., 1996b. Modeling evapotranspiration and surface energy budgets across a watershed. Water Resources Research 32 (8), 2539–2548.

Flerchinger, G.N., Kustas, W.P., Weltz, M.A., 1998. Simulating surface energy fluxes and radiometric surface temperatures for two arid vegetation communities using the SHAW model. Journal of Applied Meteorology 37 (5), 449–460.

Green, I.R.A., Stephenson, D., 1986. Criteria for comparison of single event models. Hydrological Science Journal 31, 395–411.

Hardegree, S.P., Flerchinger, G.N., Van Vactor, S.S., 2003. Hydrothermal germination response and the development of probabilistic germination profiles. Ecological Modelling 167, 305–322.

Hayhoe, H.N., 1994. Field testing of simulated soil freezing and thawing by the SHAW model. Canadian Agricultural Engineering 36 (4), 279–285.

Hymer, D.C., Moran, M.S., Keefer, T.O., 2000. Soil water evaluation using a hydrologic model and calibrated sensor network. Soil Science Society of America Journal 64 (1), 319–326.

Kennedy, I., Sharratt, B., 1998. Model comparisons to simulate frost depth. Soil Science 163 (8), 636–645.

McDonald, E.V., 2002. Numerical simulations of soil water balance in support of revegetation of damaged military lands in arid regions. Arid Land Research and Management 16, 277–290.

Nash, J.E., Sutcliffe, J.V., 1970. River flow forecasting through conceptual models: Part I—a discussion of principles. Journal of Hydrology 44, 282–290.

Parkin, G.W., Wagner-Riddle, C., Fallow, D.J., Brown, D.M., 1999. Estimated seasonal and annual water surplus in Ontario. Canadian Water Resources Journal 24, 277–292.

Pierson, F.B., Wight, J.R., 1991. Variability of near-surface soil temperature on sagebrush rangeland. Journal of Range Management 44, 491–497.

Roundy, B.A., Call, C.A., 1988. Revegetation of arid and semiarid rangelands. In: Tueller, P.T. (Ed.), Vegetation Science Applications for Rangeland Analysis and Management. Kluwer Academic Publishers, Boston, pp. 607–635.

Saxton, K.E., Rawls, W.J., Romberger, J.S., Papendick, R.I., 1986. Estimating generalized soil water characteristics from texture. Soil Science Society of America Journal 50 (4), 1031–1036.

Xu, X., Nieber, J.L., Baker, J.M., Newcomb, D.E., 1991. Field testing of a model for water flow and heat transport in variably saturated, variably frozen soil. Transportation Research Record No. 1307, Transportation Research Board, National Research Council, Washington, DC, pp. 300–308.

Young, J.A., Longland, W.S., 1996. Impact of alien plants on Great Basin rangelands. Weed Technology 10, 384–391.